

Evolution and structure formation of the distribution of partition function zeros: Triangular type Ising lattices with cell decoration

Tsong-Ming Liaw,^{1,2} Ming-Chang Huang,¹ Yen-Liang Chou,¹ and Simon C. Lin^{1,2,3}

¹*Department of Physics, Chung-Yuan Christian University, Chungli 320, Taiwan*

²*Computing Center, Academia Sinica, Nankang 115, Taiwan*

³*Institute of Physics, Academia Sinica, Nankang 115, Taiwan*

(Received 6 March 2002; published 25 June 2002)

The distribution of partition function zeros of the two-dimensional Ising model in the complex temperature plane is studied within the context of triangular decorated lattices and their triangle-star transformations. Exact recursion relations for the zeros are deduced for the description of the evolution of the distribution of the zeros subject to the change of decoration level. In the limit of infinite decoration level, the decorated lattices essentially possess the Sierpiński gasket or its triangle-star transformation as the inherent structure. The positions of the zeros for the infinite decorated lattices are shown to coincide with the ones for the Sierpiński gasket or its triangle-star transformation, and the distributions of zeros all appear to be a union of infinite scattered points and a Jordan curve, which is the limit of the scattered points.

DOI: 10.1103/PhysRevE.65.066124

PACS number(s): 64.60.Ak, 05.70.Jk

I. INTRODUCTION

Along with the intensive investigations of the two-dimensional Ising model defined on classical lattices such as the rectangular, triangular, and hexagonal lattices, some attention has been paid to the model defined on more complicated lattices. One of them is the spin model on hierarchical lattices [1–9]. These lattices are constructed as the infinite limit of a given decoration process which can be either a bond or a cell decoration. Diamond hierarchical lattice is an example of bond decorations. Starting with a bond, a diamond hierarchical lattice is obtained by replacing the bond by a diamond and then repeating the process iteratively to the infinite limit. On the other hand, Sierpiński carpet is an example of cell decorations. Starting with a square, we can construct the hierarchical lattice of a Sierpiński carpet by first dividing the square into nine equal squares, then pulling out the middle square, and finally repeating the process iteratively to the infinite limit. Since these lattices are decorated to the infinite level in a self-similar way, they are fractal lattices, and the thermodynamic limit is well defined for a physical system defined on these lattices.

Gerfen and co-workers investigated the Ising criticality on fractal lattices, including Koch curves, and Sierpiński gaskets and carpets, by means of the renormalization technique [10–13]. These authors came to the conclusion that the phase transition can occur at finite temperature only when the order of ramification of a fractal lattice is infinite [11]. There also exist some calculations on the partition functions of the Ising models on different fractal lattices embedded in two or three dimensions, and the calculation results are consistent with the above conclusion [14,15].

On the other hand, the interest about the geometric distribution of the partition function zeroes has also been raised after the classical works of Yang and Lee on regular lattices [16,17]. The Lee-Yang circle theorem states that, for the lattice gas in the thermodynamic limit, the zeros of the grand partition function are continuously distributed on a unit

circle in the complex fugacity plane, and the zero located at the real axis represents the phase transition point [16,17]. Fisher then studied the partition function zeros in the complex temperature plane, also referred as the Fisher zeros, for the two-dimensional zero-field Ising model. He showed that, for the model defined on a square lattice, the zeros lie on two circles in the complex $\tanh \eta$ plane, where $\eta = J/k_B T$ with the spin-spin coupling strength J and the Boltzmann constant k_B [18]. In principle, by knowing the zeros of the partition function, we may deduce all the thermodynamic characteristics of a system. Particularly, the distribution density of the zeros near the phase transition point can be used to extract the critical exponents [19–21]. For example, the logarithmic singularity of the specific heat for the two-dimensional zero-field Ising model is the result of the linearly vanishing density of the zeros near the real axis [18,21].

In the efforts of understanding the distribution and structure of the Fisher zeros, the zeros for the zero-field q -state Potts model has also been calculated for several values of q on the regular [20,22] as well as hierarchical lattices [6,7]. Among these results, due to the connection with the Julia set, we have fairly complete information about the Fisher zeros of hierarchical models, including the multifractal structure appearing in the distribution of the zeros and the characterization of the global scaling properties in this structure [23–25].

Fractal lattices can be viewed as the infinite limit of a certain type of hierarchical decorations starting with either a bond or a cell. Then, the renormalization approximation of Migdal [26] and Kadanoff [27] becomes exact, and the zeros of the $(n-1)$ th decoration level become the preimages of the renormalization map, which yield the zeros of the n th level. Thus, the formation of the fractal structure in the distribution of the zeros can be realized via the gradual increase of the decoration level toward the infinite limit. But, due to the fact that the number of the zeros is finite for a finite decoration level, we cannot show how the fractal structure emerges from the increase of the decoration level in a clear

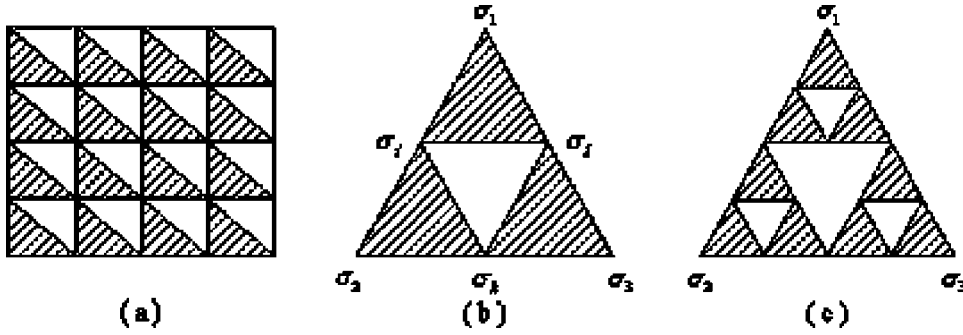
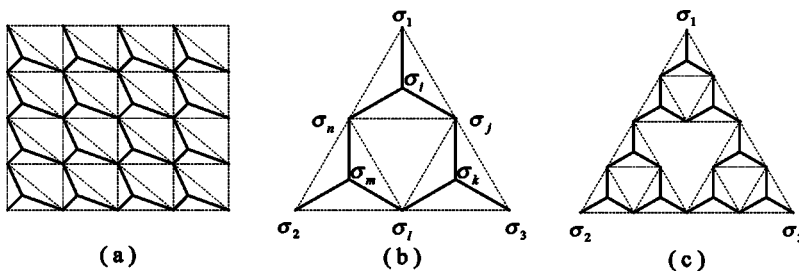


FIG. 1. (a) A triangular lattice consists of primary cells (shaded region). A primary cell is decorated to (b) one level and (c) two levels. Note that σ_1 , σ_2 , and σ_3 are the corner spins and the others are inner spins.

way. However, this can be improved if lattices possessed a well-defined thermodynamic limit for any decoration level in the passage toward a fractal lattice.

To construct a hierarchically decorated lattice that has a well-defined thermodynamic limit for any degree of decorations, we can start with a classical regular lattice, and then implement bond or cell decorations hierarchically to this lattice to any desired degree. In the limit of infinite decoration level, the decorated lattice essentially possesses the fractal lattice as the inherent structure. For decorated lattices constructed in this way, they show lack of translational invariance, and the degree of inhomogeneity in the coordination number of lattice sites can be indexed by the number of the decoration level. Thus, one may expect that this type of lattices may provide a very good frame to deepen our understanding of physical systems such as random magnets, polymers, and percolation clusters.

Using these decorated lattices, we attempt to give a systematic study of the effect of inhomogeneity on the thermodynamic behavior of the two-dimensional zero-field Ising model. This is the first of two papers that study the evolution and structure formation of the Fisher zeros on decorated lattices with an arbitrary decoration level n (n lattice, hereafter). In this paper, we study the model defined on a triangular and hexagonal lattice with cell decorations, while the model on a rectangular lattice with bond decorations is studied in the second paper. We are interested in the following questions. (i) How do the critical point and the distribution of the Fisher zeros vary with the decoration level n ? (ii) How does the fractal structure in the distribution of the Fisher zeros emerge from the increase of the decoration level? (iii) Is there any difference for the fractal structure in the distribution of the Fisher zeros between a fractal lattice and a decorated lattice with the fractal lattice as the inherent structure? The question of how the specific heat on an n lattice varies with the decoration level n will be discussed in other separated papers.



II. FREE ENERGY

In this paper, two kinds of regular lattices are chosen for decoration: One is planar triangular lattice shown in Fig. 1(a), and the other is hexagonal lattice, which is obtained from the last one by a triangle-star transformation shown in Fig. 2(a). For the way of generating hierarchical decorations, we adopt the rule depicted in Fig. 1 for a triangular lattice, and its corresponding triangle-star transformation to a hexagonal lattice is shown in Fig. 2. In the limit of infinite decoration level, the decorated lattices essentially possess the Sierpiński gasket and its triangle-star transformation as the inherent structure for the triangular and hexagonal lattice, respectively. The corresponding site number $N_s^{(n)}$ and the bond number $N_b^{(n)}$ per unit cell of regular lattices (referred as primary cell, hereafter) for the decoration level n are $(3^{n+1} - 1)/2$ and 3^{n+1} for a triangular decorated lattice, and $(5 \times 3^n - 1)/2$ and 3^{n+1} for a hexagonal decorated lattice.

The general form of the partition function reads

$$Z = \sum_{\{\sigma_i\}} \exp\left(\sum_{\langle i,j \rangle} \zeta \sigma_i \sigma_j\right), \quad (1)$$

where the sum is over the nearest neighboring pairs $\langle i,j \rangle$ on a certain type of hierarchically decorated lattices. Here we consider uniform ferromagnetic couplings characterized by the dimensionless coupling parameter η , and the Ising spin takes two possible values $\sigma_i = \pm 1$. Formally, the exponential part of Eq. (1) can be rewritten as simple products, and this renders the partition function to be

$$Z = 2^{n_s} R^{n_b} Q, \quad (2)$$

with $R = (1 - t^2)^{-1/2}$ and $t = \tanh \eta$, where n_s and n_b are the total site and bond numbers respectively, and the reduced partition function Q takes the form of

FIG. 2. (a) A hexagonal lattice is obtained from a triangle-star transformation. A primary cell decorated to (b) one level and (c) two levels in a triangular lattice is transferred to a hexagonal lattice through the triangle-star transformation. Note that σ_1 , σ_2 , and σ_3 are the corner spins on the corresponding primary cell of a hexagonal lattice.

$$Q = \left(\frac{1}{2} \right)^{n_s} \sum_{\sigma = \pm 1} \left\{ \prod_{\langle i,j \rangle} (1 + t \sigma_i \sigma_j) \right\}. \quad (3)$$

The expression of Q in all cases can be unified by means of the characteristic spin functional defined on a primary cell, this formally leads to

$$Q = \left(\frac{1}{2} \right)^{n_s/N_s} \sum_{\sigma = \pm 1} \left\{ \prod_{\text{cells}} A_{1,2,3} \right\} \quad (4)$$

with

$$A_{1,2,3} = \alpha + \beta(\sigma_1 \sigma_2 + \sigma_2 \sigma_3 + \sigma_3 \sigma_1), \quad (5)$$

where the product is taken over all the primary cells, the spin variables, σ_1, σ_2 and σ_3 , are the corner spins on the primary cell for the construction depicted in Figs. 1 and 2, and α and β are certain defined functionals of the variable t . Note that for the zero-field Ising model with the nearest neighbor interactions, the characteristic spin functional $A_{1,2,3}$ always takes bilinear form of the spin variables, and the functional coefficients before three different spin-pairs are the same for the case of uniform couplings.

For the case of the zeroth order decoration, the corresponding functional coefficients, α and β , in the characteristic spin functional $A_{1,2,3}$ of Eq. (4) can be calculated from simple relations,

$$\begin{aligned} \alpha_T^{(0)} + \beta_T^{(0)}(\sigma_1 \sigma_2 + \sigma_2 \sigma_3 + \sigma_3 \sigma_1) \\ = (1 + t \sigma_1 \sigma_2)(1 + t \sigma_2 \sigma_3)(1 + t \sigma_3 \sigma_1), \end{aligned} \quad (6)$$

$$\begin{aligned} \alpha_H^{(0)} + \beta_H^{(0)}(\sigma_1 \sigma_2 + \sigma_2 \sigma_3 + \sigma_3 \sigma_1) \\ = \frac{1}{2} \sum_{\sigma_0} (1 + t \sigma_1 \sigma_0)(1 + t \sigma_2 \sigma_0)(1 + t \sigma_3 \sigma_0), \end{aligned} \quad (7)$$

which yield

$$\alpha_T^{(0)} = 1 + t^3, \quad (8)$$

$$\beta_T^{(0)} = t(1 + t), \quad (9)$$

$$\alpha_H^{(0)} = 1, \quad (10)$$

$$\beta_H^{(0)} = t^2. \quad (11)$$

Here the subscripts T and H denote the triangular and hexagonal lattices, and superscripts with parenthesis denote the decoration level.

For a lattice with the decoration level n , the functional coefficients $\alpha^{(n)}$ and $\beta^{(n)}$ can be obtained through the recursion relations between two successive decoration levels. An effective way of constructing these recursion relations is to patch three of the neighboring ancestor lattices together and then to complete the sum over the inner spins. In this construction, the characteristic spin functional at the decoration levels $n, A_{1,2,3}^{(n)}$, can be expressed in terms of those at the decoration levels $n-1, A_{i,j,k}^{(n-1)}$, as

$$A_{1,2,3}^{(n)} = \left(\frac{1}{2} \right)^3 \sum_{\{\sigma_i, \sigma_j, \sigma_k\}} \{A_{1,i,j}^{(n-1)} A_{i,2,k}^{(n-1)} A_{j,k,3}^{(n-1)}\}, \quad (12)$$

which appears to preserve the form of Eq. (5) after taking averaged sums over the inner spins, σ_i, σ_j , and σ_k . Hence the associated recursion relations of the functional coefficients are given as

$$\alpha^{(n)} = (\alpha^{(n-1)})^3 + (\beta^{(n-1)})^3, \quad (13)$$

$$\beta^{(n)} = (\beta^{(n-1)})^2 (\alpha^{(n-1)} + \beta^{(n-1)}) \quad (14)$$

for both lattices T and H .

The above results indicate that the characteristic spin functional $A_{1,2,3}^{(n)}$ does preserve its form as

$$A_{1,2,3}^{(n)} = \alpha^{(n)} + \beta^{(n)}(\sigma_1 \sigma_2 + \sigma_2 \sigma_3 + \sigma_3 \sigma_1) \quad (15)$$

in any decoration levels n . Then the reduced partition function for a lattice with n decoration levels takes the general form of

$$\begin{aligned} Q^{(n)} = \left(\frac{1}{2} \right)^{N_s^{(n)}} \sum_{\sigma = \pm 1} \left\{ \prod_{x,y} [\alpha^{(n)} + \beta^{(n)}(\sigma_{x,y} \sigma_{x+1,y} \right. \\ \left. + \sigma_{x,y} \sigma_{x,y+1} + \sigma_{x+1,y} \sigma_{x,y+1})] \right\}, \end{aligned} \quad (16)$$

where the two-tuple (x, y) in the subscript of a spin variable denotes the position of an Ising spin located at one of the sites in a lattice with the zeroth order decoration.

Since, the reduced partition function of decorated lattices stays unaltered up to certain well-defined functional coefficients, the system is completely resolved, and the free energy can be easily written down according to the formal expression of exact solution provided by Refs. [28–30]. The expression of the free energy per site per $k_B T$ can be written as the sum of two parts,

$$f^{(n)} = f_r^{(n)} + f_s^{(n)}, \quad (17)$$

where $f_r^{(n)}$ is the regular part,

$$f_r^{(n)} = -\ln 2 - \frac{N_b^{(n)}}{N_s^{(n)}} \ln R, \quad (18)$$

and $f_s^{(n)}$, coming from the reduced partition function $Q^{(n)}$, is the singular part,

$$f_s^{(n)} = \frac{-1}{2N_s^{(n)}} \int_0^{2\pi} d\phi \int_0^{2\pi} d\theta \frac{1}{2\pi} \ln [B_0^{(n)} - B_1^{(n)} \Theta(\theta, \phi)], \quad (19)$$

with $B_0^{(n)}$ and $B_1^{(n)}$ defined as

$$B_0^{(n)} = (\alpha^{(n)})^2 + 3(\beta^{(n)})^2, \quad (20)$$

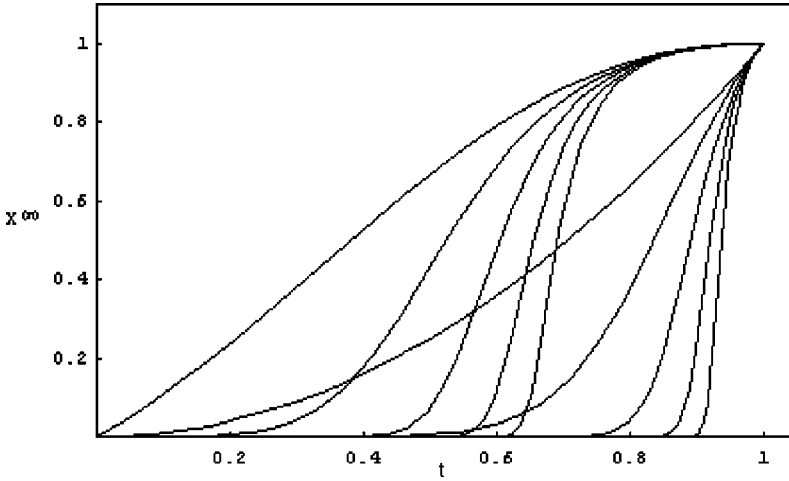


FIG. 3. The quantity $X^{(n)}$, defined as $X^{(n)} \equiv \beta^{(n)}/\alpha^{(n)}$, as a function of t decreases rapidly to zero as the decoration level n increases for triangular (black) and hexagonal (gray) decorated lattices, with $n=0,2,4,6$ and 10 from left to right.

$$B_1^{(n)} = 2[\alpha^{(n)}\beta^{(n)} - (\beta^{(n)})^2], \quad (21)$$

and $\Theta(\theta, \phi)$ defined as

$$\Theta(\theta, \phi) = \cos \theta + \cos \phi + \cos(\theta - \phi). \quad (22)$$

It is interesting to consider the lattice formed by an isolated primary cell with the decoration level n , which leads to a conventional fractal lattice in the limit of infinite n . After summing over the three corner spins σ_1 , σ_2 , and σ_3 , we obtain the singular part of the free energy density as

$$f_{s,cell}^{(n)} = -\frac{1}{N_s^{(n)}} \ln \alpha^{(n)}. \quad (23)$$

On the other hand, by introducing new variables $X^{(n)} \equiv \beta^{(n)}/\alpha^{(n)}$, we can rewrite the singular part of the free energy density given by Eq. (19) as

$$f_s^{(n)} = \frac{-1}{2N_s^{(n)}} [2 \ln \alpha^{(n)} + C^{(n)}(t)], \quad (24)$$

where $C^{(n)}(t)$ is the result of the integration defined as

$$C^{(n)}(t) = \int_0^{2\pi} \frac{d\phi}{2\pi} \int_0^{2\pi} \frac{d\theta}{2\pi} \ln \{ (1 + 3X^{(n)}) - 2[X^{(n)} - (X^{(n)})^2] \Theta(\theta, \phi) \}. \quad (25)$$

Then, by comparing Eq. (24) with Eq. (23) we know that the quantity $C^{(n)}(t)$ signifies the contribution to the free energy density from the correlations among different primary cells.

From the recursion relations of Eqs. (13) and (14), we can obtain the recursion relation of $X^{(n)}$ as

$$X^{(n)} = \frac{(X^{(n-1)})^2}{1 - X^{(n-1)} + (X^{(n-1)})^2}. \quad (26)$$

This map between two successive decoration levels has two fixed points, one at $X_f = 1$ is repulsive and the other at $X_f = 0$ is attractive. Note that we can determine a fixed point, $X_f = 1$ or 0 , to be repulsive or attractive by directly observ-

ing that the value of $X^{(n)}$ is a decreasing sequence in the increase of the decoration levels n for a given t value between 0 and 1 . Hence, the increase of the decoration levels n will decrease the value of $X^{(n)}$ down to $X^{(n)} = 0$ for any t value except the point $t = 1$ that corresponds to the repulsive fixed point $X_f = 1$. This feature is shown in Fig. 3. Hence, we have the integration result $C^{(n)}(t)$ of Eq. (25) vanish in the range $0 < t < 1$ for the infinite decoration level, and then the free energy density of Eq. (24) is the same as that of the decoupled primary cells.

Thus, decorations play the role of weakening the correlations among the primary cells, and eventually there is no phase transition at finite temperature when the decoration levels n is sufficiently large.

III. CRITICAL POINT

In view of the dimensionless free energy density given by Eq. (19), the bulk critical temperature for the ferromagnetic phase transition is determined by the condition [28,30]

$$B_0^{(n)} - 3B_1^{(n)} \stackrel{c}{=} 0, \quad (27)$$

where, for convenience, we use the notation, $\stackrel{c}{=}$, to denote the equivalence established only at the critical temperature. In principle, Eq. (27) has to be converted into the relations of the variable t and to be solved with respect to the variable t for a lattice with decoration levels n . But as the decoration level goes higher, the relevant functionals, $B_0^{(n)}$ and $B_1^{(n)}$, become extremely complicated in the variable t , and it is not easy to determine the critical temperature accurately. Therefore, we consider seeking an analytical way to reformulate the critical condition of Eq. (27).

In view of the recursion relations of Eqs. (13) and (14), we can introduce more appropriate variables to manage the critical condition. For the ratio of the functional coefficients, $Y^{(n)} \equiv 1/X^{(n)} = \alpha^{(n)}/\beta^{(n)}$, the recursion relation take the form of

$$Y^{(n)}(t) = Y^{(n-1)}(t)[Y^{(n-1)}(t) - 1] + 1. \quad (28)$$

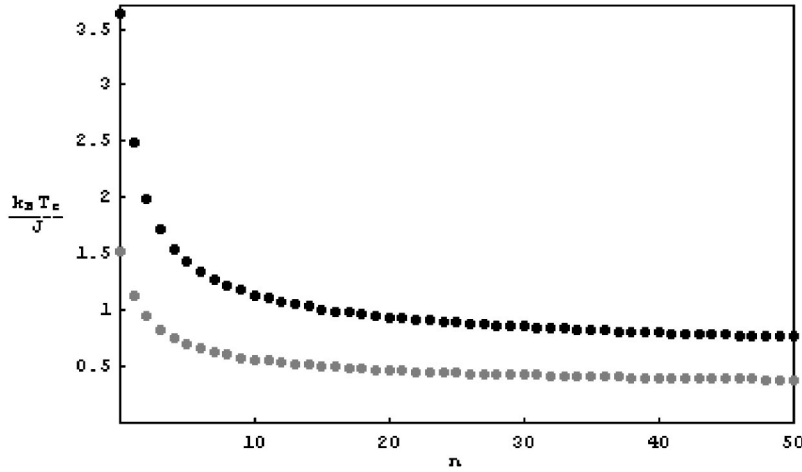


FIG. 4. The critical points $k_B T_c / J$ vs the decoration level n for triangular (black) and hexagonal (gray) decorated lattices.

Then, in terms of the new variable Y , the critical condition of Eq. (27) can be reduced to the form of

$$Y^{(n)}(t) \stackrel{c}{=} h^{(0)}, \quad (29)$$

with $h^{(0)} = 3$.

To solve the critical condition of Eq. (29), first we use Eq. (28) to rewrite it as

$$Y^{(n-1)}(t)[Y^{(n-1)}(t) - 1] + 1 \stackrel{c}{=} h^{(0)}, \quad (30)$$

which, in general, has two roots,

$$Y^{(n-1)}(t) \stackrel{c}{=} \frac{1}{2} (1 \pm \sqrt{4h^{(0)} - 3}). \quad (31)$$

However, one of the solutions, $(1 - \sqrt{4h^{(0)} - 3})/2$, must be disregarded due to the fact that this root appears to be negative in the physical region, $0 < t < 1$, while the left hand side of Eq. (31) is essentially positive definite for the ferromagnetic couplings. Then we can rewrite Eq. (29) as

$$Y^{(n-1)}(t) \stackrel{c}{=} h^{(1)}, \quad (32)$$

with $h^{(1)}(t) = (1 + \sqrt{4h^{(0)} - 3})/2$. Hence, by further reductions we can expect

$$Y^{(n-i)}(t) \stackrel{c}{=} h^{(i)}, \quad (33)$$

with

$$h^{(i)} = \frac{1}{2} (1 + \sqrt{4h^{(i-1)} - 3}), \quad (34)$$

for $1 \leq i \leq n$.

When Eq. (33) is applied to a lattice with decoration levels n , this equation with any i value in the range $1 \leq i \leq n$ is equivalent to Eq. (29), and this equivalence can be viewed as a kind of renormalization scheme for the critical point subject to the size changing inside the lattice. It corresponds to rescaling the system to the low momentum limit when the i value increases.

Then the critical value of the hyperbolic tangential function $t_c = \tanh \eta_c$, and hence the critical temperature, can be

determined by solving Eq. (33) for any i value. The most convenient way of doing this is to handle the last expression of Eq. (33)

$$Y^{(0)} \stackrel{c}{=} h^{(n)}, \quad (35)$$

since $Y^{(0)}$ is a simple function of t for both lattices T and H and $h^{(n)}$ is a constant number regardless of the n value. By using the recursion relation of Eq. (34) with the initial $h^{(0)} = 3$, we can obtain the constant value $h^{(n)}$ for any decoration level n . Then, for the decoration level n we solve Eq. (35) with $Y^{(0)} = (1 - t + t^2)/t$ for the lattice T to obtain the critical point $t_{c,T}$ as

$$t_{c,T} = \frac{(h^{(n)} + 1) - \sqrt{(h^{(n)} + 3)(h^{(n)} - 1)}}{2}, \quad (36)$$

and with $Y^{(0)} = 1/t^2$ for the lattice H to obtain the critical point $t_{c,H}$ as

$$t_{c,H} = \frac{1}{\sqrt{h^{(n)}}}. \quad (37)$$

The numerical values of $t_{c,T}$ and $t_{c,H}$ versus the decoration level n are shown in Fig. 4.

As stated above, the critical point can be determined by solving Eq. (35) in conjunction with the recursion relation of Eq. (34). Thus, for the case of n approaching infinity, in order to determine the corresponding critical temperature we have to know the asymptotic behavior of the function $h^{(n)}$ as n goes to ∞ . Concerned with the sequence built up by the functions $h^{(n)}$ of increasing n , one may find that the values decrease uniformly for any t value of interest. On the other hand, we recall that all $h^{(i)}$'s must be strictly real and positive according to the construction of Eq. (33) and the physical requirement. Thus, $h^{(n)}$ stays positive and it is bounded below, accumulation points do exist and they can be obtained via a fixed point equation

$$h^{(\infty)} = \frac{1}{2} (1 + \sqrt{4h^{(\infty)} - 3}), \quad (38)$$

which yields $h^{(\infty)} = 1$ for both lattices T and H .

By virtue of Eqs. (36) and (37), direct substitution of $h^{(\infty)}=1$ leads to the result $t_{c,T}=t_{c,H}=1$ for the infinite decoration level. Therefore, we may conclude that there are no phase transitions at finite temperatures for these cases, and this result is consistent with the conclusion given by Gerfen *et al.*

IV. PARTITION FUNCTION ZEROS

In this section, we focus on the distribution of the Fisher zeros for an arbitrary n lattice and how the fractal structure emerge in the distribution for the limit of infinite n . In general, the Fisher zeros can be obtained by simply setting the argument of the logarithm in the singular part of the free energy density of Eq. (19) equal to zero. In terms of the variable $Y^{(n)}$, Eq. (19) takes the form of

$$f_s^{(n)} = \frac{-1}{2N_s^{(n)}} \left(2 \ln \beta^{(n)} + \int_0^{2\pi} \frac{d\phi}{2\pi} \int_0^{2\pi} \frac{d\theta}{2\pi} \ln \{ [3 + (Y^{(n)})^2] - 2(Y^{(n)} - 1)\Theta(\theta, \phi) \} \right). \quad (39)$$

Thus, the distribution of the zeros can be resolved as a union of the solutions from the two conditions as

$$[3 + (Y^{(n)})^2] - 2(Y^{(n)} - 1)\Theta(\theta, \phi) = 0 \quad (40)$$

and

$$\beta^{(n)} = 0. \quad (41)$$

Concerned with Eq. (40), we observe that the range of the function $\Theta(\theta, \phi)$ is $-3/2 \leq \Theta(\theta, \phi) \leq 3$. For that $-1 \leq \Theta(\theta, \phi) \leq 3$, the condition of Eq. (40) is equivalent to $|Y^{(n)} - 1| = 2$, which corresponds to a circle of radius 2 with the center being located at 1 on the $Y^{(n)}$ complex plane. On the other hand, the range of $-3/2 \leq \Theta(\theta, \phi) \leq -1$ gives the line segment $[-3, 0]$ on the real axis. Hence, the solution of Eq. (40) leads to the distribution of the zeros as a circle plus a line segment on the $Y^{(n)}$ complex plane for an n lattice as shown in Fig. 5(a). It is worthwhile to note that this result is consistent with the results for 0 lattice obtained elsewhere [19,21].

However, for an effective comparison of the distributions of the zeros given at any decoration level, the plots had better to be brought to the complex plane of a unique variable $Y^{(0)}$, which corresponds to different function of t for the lattices T and H . To achieve this, we notice that knowing the zeros distribution on the $Y^{(n)}$ complex plane we can obtain the distribution on the $Y^{(0)}$ complex plane by performing the inverse map of Eq. (28), given as

$$Y^{(n-1)} = \frac{1}{2} \pm \frac{\sqrt{4Y^{(n)} - 3}}{2}, \quad (42)$$

consecutively n times. We also notice that on the $Y^{(0)}$ complex plane, as a consequence of the Lee-Yang theorem

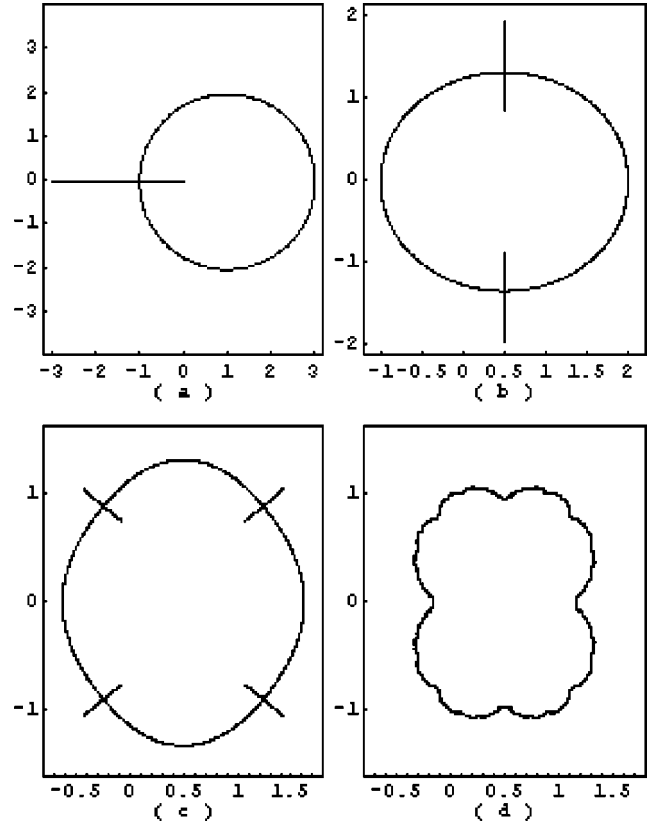


FIG. 5. The distribution of the partition function zeros on the $Y^{(0)}$ complex plane obtained from the solution of Eq. (40) for the decoration level (a) $n=0$, (b) $n=1$, (c) $n=2$, and (d) $n=8$.

[16,17], the critical point, given by $Y^{(0)}=h^{(n)}$, corresponds to the only zero located at the physical region $1 < Y^{(0)} < \infty$ with real $Y^{(0)}$ for an n lattice.

On the $Y^{(n)}$ complex plane, the distribution of the zeros for an n -lattice, obtained from Eq. (40), is a circle and a line segment, and there is an intersection point between the circle and the line segment located at the point $Y^{(n)} = (-1, 0)$. As is depicted in Fig. 5(b), after the first inverse map, the circle shrinks but remains closed, whereas the line segment splits into two curved segments that intersect with the closed curve at the points determined by the inverse map of the last intersection $(-1, 0)$. The resultant distribution, which is the union of a closed curve and two curved segments, has the space inversion symmetry about the symmetric center $Y^{(n-1)} = (0.5, 0)$. For convenience, we shall call the closed curve as $(n-1)$ cycle and, in this sense, the original circle can be named as n cycle.

Proceeding with the second inverse map, as shown in Fig. 5(c), the $(n-1)$ cycle further shrinks to another closed curve, the $(n-2)$ cycle, meanwhile, the two curved segments split into four shortened ones. Therefore, the resultant pattern for the zeros in the complex $Y^{(n-2)}$ plane possesses the $(n-2)$ cycle as well as the four curved segments. Here, the distribution maintains the space inversion symmetry about the point $(0.5, 0)$, and the four intersections between the $(n-2)$ cycle and the four segments are the resultant points of the inverse map, given by Eq. (42), of the two

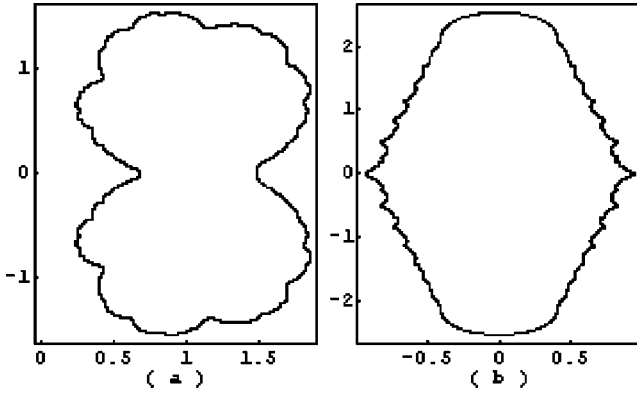


FIG. 6. The distribution of the partition function zeros on the t complex plane obtained from Eq. (40) for (a) triangular and (b) hexagonal decorated lattices with the decoration level $n=8$.

intersections between the $(n-1)$ cycle and the two curved segments on the $Y^{(n-1)}$ complex plane.

In general, for an n lattice, the distribution of the zeros subject to the solutions of Eq. (40) is the union of an $(n-i)$ cycle and 2^i separated curved segments on the $Y^{(n-i)}$ complex plane. In this distribution, there are 2^i intersection points between the $(n-i)$ cycle and 2^i separated curved segments, and these intersections are the results of the inverse map, given by Eq. (42), of the $2^{(i-1)}$ intersections between the $[n-(i-1)]$ cycle and 2^{i-1} separated curved segments on the $Y^{[n-(i-1)]}$ complex plane. In addition, this distribution has the space inversion symmetry about the symmetric center $(0.5,0)$.

Then, it is obvious that for an n lattice, the distribution of the zeros on the $Y^{(0)}$ complex plane contains a 0 cycle and 2^n segments, and this 0 cycle is a continuous curve that is characterized by its 2^n intersection point with 2^n segments. For sufficiently large n , the lengths of the 2^n segments become tiny and the 2^n intersection points turns out to dominate the 0 cycle, as depicted in Fig. 5(d) for the case of $n=8$. In the limit where n tends to infinity, these segments have shrunk to the 2^n points which then solely determine the 0 cycle. Therefore, for an n lattice with n approaching the infinity, the solution of Eq. (40) gives the distribution of the zeros in the complex $Y^{(0)}$ plane as the set of infinite points for both T and H structures. Owing to the fact that the map given by Eq. (28), up to a constant translation, can be identified as one of the rational maps, $z \rightarrow z^2 + c$ with $c=1/4$, this set of infinite points, which is also referred as the Jordan curve in the literature, is a Julia set [31]. For reference, we also show the zeros distribution from the solution of Eq. (40) on the t complex plane for T structure in Fig. 6(a) and for H structure in Fig. 6(b), both with the decoration level $n=8$.

For the condition of Eq. (41), $\beta^{(n)}=0$, because of the definition of $B_1^{(n)}$ given by Eq. (21) this condition essentially leads to $B_1^{(n)}=0$, and, hence, $B_0^{(n)}=0$ by virtue of the condition for the zeros, $B_0^{(n)} - B_1^{(n)} \Theta(\theta, \phi) = 0$. Therefore, Eq. (41), actually, implies $\alpha^{(n)} = \beta^{(n)} = 0$ as a consequence of $B_0^{(n)} = B_1^{(n)} = 0$. Using the recursion relations (13) and (14), we obtain two conditions, $Y^{(n-1)} = -1$ and $\alpha^{(n-1)} = \beta^{(n-1)} = 0$, which are equivalent to the condition $\alpha^{(n)} = \beta^{(n)} = 0$ for

an n lattice. By continuing the reduction always along the branch $\alpha^{(m)} = \beta^{(m)} = 0$, eventually we can decompose the condition for the zeros, Eq. (41), into the following:

$$Y^{(n-i)} = -1, \quad \text{for } i=1, \dots, n, \quad (43)$$

and

$$\alpha^{(0)} = \beta^{(0)} = 0. \quad (44)$$

The last condition cannot be satisfied for lattice H , and it implies $t = -1$ or $Y^{(0)} = -3$ for lattice T . Hence, for an n lattice the condition of Eq. (41) yields the zeros on the $Y^{(0)}$ complex plane as the union of the point $(-3,0)$ (this point is absent for lattice H), the points obtained from the result of performing the inverse map, given by Eq. (42), $n-1$ times successively for the point -1 , and all the preimages in those $n-1$ times inverse maps.

Recall that for the solution of Eq. (40), the point $Y^{(n-1)} = (-1,0)$ is the intersection point between the $(n-1)$ cycle and the line segment on the $Y^{(n-1)}$ complex plane for a $(n-1)$ lattice. For the case of infinite n , this point generates all the points of the Julia set on the $Y^{(0)}$ complex plane through the inverse map of Eq. (42) consecutively. Thus, for the case of infinite n , the solution of Eq. (40) is a subset of the solution of Eq. (41), and the distribution of the zeros is solely determined by the condition of Eq. (41). This result is consistent with the conclusion we obtained from the comparison of the singular part of the free energy density between an n lattice and a isolated primary cell with the decoration level n , namely, decorations play the role of weakening the correlations among the primary cells.

By combining the solutions of Eqs. (40) and (41) together, we may conclude that for an n lattice the Fisher zeros in the complex $Y^{(0)}$ plane consist of a 0 cycle, 2^n separated curved segments that intersect the 0 cycle at different points determined by the n times inverse map of the point $(-1,0)$, and the scattered points including the point $(-3,0)$, which is absent for lattice H , the points obtained from the result of performing the inverse map of Eq. (42) $n-1$ times successively for the point $(-1,0)$, and all the preimages in those $n-1$ times inverse maps.

V. SUMMARY

In summary, an exact cell-renormalization transformation were constructed and used to study the critical points and the Fisher zeros for the Ising model on triangular type lattices with cell decorations. We exactly locate the critical point for an n lattice with arbitray n , and show that there is no phase transition at finite temperature for the infinite decoration level. For the distribution of the Fisher zeros, we choose a unique variable as the variable of complex temperature, and then we bring the zeros distributions for lattices with different decoration levels to this complex plane so that the patterns of the distributions can be compared with each other. The pattern first appears as a union of a circle and a line segment for lattices without decorations. Then, as the decoration level increases, the pattern gradually evolves to a set of scattered points limited by a Jordan curve in the limit of

infinite decoration level. By direct construction of the evolution process, we can show the emergence of the fractal structure of the Jordan curve in a clear way. We also show that the Sierpiński gasket essentially possesses the same distribution of the zeros as the triangular lattice with the inherent structure of the Sierpiński gasket. This is shown to be due to the fact that each primary cell tempts to factorize from the sys-

tem when the decoration levels increase, and a complete factorization occurs in the limit of infinite decoration levels.

ACKNOWLEDGMENT

This work was partially supported by the National Science Council of ROC (Taiwan) under Grant No. NSC 89-2112-M-033-004.

-
- [1] R.B. Griffiths and M. Kaufman, *Phys. Rev. B* **26**, 5022 (1982).
 - [2] N.M. Svrakic, J. Kertesz, and W. Selke, *J. Phys. A* **15**, L427 (1982).
 - [3] B. Derrida, J.P. Eckmann, and A. Erzan, *J. Phys. A* **16**, 893 (1983).
 - [4] M. Kaufman and R.B. Griffiths, *Phys. Rev. B* **24**, 496 (1981).
 - [5] A. Erzan, *Phys. Lett.* **A93**, 237 (1983).
 - [6] B. Derrida, L.De. Seze, and C. Itzykson, *J. Stat. Phys.* **33**, 559 (1983).
 - [7] B. Derrida, C. Itzykson, and J.M. Luck, *Commun. Math. Phys.* **94**, 115 (1985).
 - [8] F.T. Lee and M.C. Huang, *J. Stat. Phys.* **75**, 1119 (1994).
 - [9] F.T. Lee and M.C. Huang, *Chin. J. Phys. (Taipei)* **37**, 398 (1999).
 - [10] Y. Gefen, Y. Meir, B.B. Mandelbrot, and A. Aharony, *Phys. Rev. Lett.* **50**, 145 (1983).
 - [11] Y. Gefen, B.B. Mandelbrot, and A. Aharony, *Phys. Rev. Lett.* **45**, 855 (1980).
 - [12] Y. Gefen, A. Aharony, and B.B. Mandelbrot, *J. Phys. A* **16**, 1267 (1983); **17**, 1277 (1984).
 - [13] Y. Gefen, A. Aharony, Y. Shapir, and B.B. Mandelbrot, *J. Phys. A* **17**, 435 (1984).
 - [14] Z.R. Yang, *Phys. Rev. E* **49**, 2457 (1994).
 - [15] P. Monceau, M. Perreau, and F. Hebert, *Phys. Rev. B* **58**, 6386 (1998).
 - [16] C.N. Yang and T.D. Lee, *Phys. Rev.* **87**, 404 (1952).
 - [17] T.D. Lee and C.N. Yang, *Phys. Rev.* **87**, 410 (1952).
 - [18] M. E. Fisher, *Lecture Note in Theoretical Physics*, edited by W. E. Brittin (University of Colorado Press, Boulder, 1965), Vol. 7c, pp. 1–159.
 - [19] J. Stephenson and R. Couzen, *Physica A* **129**, 201 (1984).
 - [20] H. Feldmann, R. Shrock, and S.H. Tsai, *Phys. Rev. E* **57**, 1335 (1998).
 - [21] W.T. Lu and F.Y. Wu, *J. Stat. Phys.* **102**, 953 (2001).
 - [22] C.N. Chen, C.K. Hu, and F.Y. Wu, *Phys. Rev. Lett.* **76**, 169 (1996).
 - [23] M.H. Jensen, L.P. Kadanoff, and I. Procaccia, *Phys. Rev. A* **36**, 1409 (1987).
 - [24] B. Hu and B. Lin, *Phys. Rev. A* **39**, 4789 (1989).
 - [25] B. Hu and B. Lin, *Physica A* **177**, 38 (1991).
 - [26] A.A. Migdal, *Sov. Phys. JETP* **42**, 743 (1976).
 - [27] L.P. Kadanoff, *Ann. Phys. (N.Y.)* **100**, 359 (1976).
 - [28] V.N. Plechko, *Physica A* **152**, 51 (1988).
 - [29] V.N. Plechko and I.K. Sobolev, *Phys. Lett. A* **157**, 335 (1991).
 - [30] T.M. Liaw, M.C. Huang, S.C. Lin, and M.C. Wu, *Phys. Rev. B* **60**, 12 994 (1999).
 - [31] K. Falconer, *Fractal Geometry: Mathematical Foundations and Applications* (Wiley, New York, 1990).